Digital Computer Simulation of a Four-Phase Data Transmission System

By M. A. RAPPEPORT

(Manuscript received June 21, 1963)

This paper discusses the performance of a four-phase data transmission system in the presence of delay distortion and impulse noise. The tool used in this investigation is digital computer simulation, including a new technique for introducing impulse noise.

The noise studies indicate the usefulness of the eye aperture for measuring the degrading effects of delay distortion on such a four-phase system. Using the eye aperture as a criterion, the effects on performance of sinusoidal, parabolic, quartic, and parabolically bounded sinusoidal delays are studied. Curves showing the resulting degradation in performance are obtained. These are used to find bounds on allowable delay for a certain allowable degradation for lines typical of equalized voice or group bandwidths, usual nonequalized voice-bands, and loaded cable type voice-bands.

I. INTRODUCTION

1.1 *Nature of Simulation and of the Telephone Plant*

Digital computer simulation can be a powerful tool in the study of data transmission systems. This paper begins with a discussion of the techniques that have proved useful in applying this tool to various data transmission systems, including a new technique for studying the effects of impulse noise. These methods are then used for a detailed simulation study of a four-phase data transmission system.

Digital computer simulation, in general, aims at studying some physical system by a mathematical model of the system on a digital computer. In particular we are concerned with a real data transmission system in a real telephone plant. The scope of this paper is thus the performance of data systems over a time-stationary transmission path chosen at random from an ensemble of such lines.

The major forms of interference which concern us are this time-

invariant transmission distortion and random additive impulse noise. Transmission distortion is characterized as nonuniform attenuation and/or nonlinear phase as a function of frequency across the transmission band of the system. Nonlinear phase is commonly characterized in terms of nonuniform envelope delay, i.e., envelope delay distortion. Impulse noise is defined here as any randomly occurring voltage (or current) disturbances characterized by the occurrence of larger numbers of high peaks or pulses of noise than would be present in Gaussian noise of the same power, interspersed with long, low-power ("quiet") periods. There are, of course, many other forms of disturbance in the telephone plant, ranging from line dropout and frequency offset to the special case of undersea cables where Gaussian background noise is the significant disturbance. While some of these factors are amenable to simulation, this paper is concerned only with the effects of transmission distortion and impulse noise.

1.2 *Reasons for Using Simulation*

The underlying reason for studying data transmission by digital computer simulation is the complexity of the data system itself. This includes the range and nature of the ensemble of possible telephone transmission facilities, difficulties both in specifying and working with impulsive type noises in closed form, and the analytic difficulties in investigating real modulators and demodulators. This complexity presents problems both in analytic and experimental approaches.

In the laboratory there are two major difficulties: first, obtaining insight into the basic workings of the system in an environment which is very difficult to control in the laboratory; second, obtaining sufficient flexibility to provide a controlled investigation of the wide range of conditions encountered in actual practice.

Whereas in the experimental approach one of the difficulties is to see the forest for the trees, the analytical approach has the problem of having to clear away too many of the trees to make the forest visible at all. That is, the analytic approach often has to make a large number of assumptions about the performance of a real system in order to make the analysis tractable in closed form. For example, analytical approaches generally substitute the more easily handled Gaussian noise for the actually present impulse noise.

It is an attempt to get the best of both worlds that leads one to simulation. One hopes that the environment and all the factors in it can be controlled, without forcing the investigator into too many simplifying

assumptions that may lead to misleading results. Because of this sort of hybrid approach, simulation has two major goals. First, insight is sought into how a system really works. Among other particular aims, one seeks the allowable assumptions that can be made in analyzing a system, the basic and secondary factors affecting system performance, possible new directions in design and so on. Second, simulation hopes to produce a catalog of the expected performance of a real system for a realistic range of transmission and noise environments.

II. SCOPE OF FOUR-PHASE RESULTS

Sections III and IV describe the simulation techniques used and the particular four-phase system considered. In this section the results obtained are briefly listed for purpose of reference. The results can be grouped in four classes: modem (modulator-demodulator) design, choice of criterion, numerical specification of performance for particular transmission conditions, and application of these numerical results to give general transmission design specifications.

The modem design results obtained (Section 5.1) are on the modulation envelope shaping. In particular, the desirable amount of overlap between successive pulses is obtained. The same results were obtained simultaneously and independently in a laboratory test of the physical system by P. A. Baker,[1] and thus are useful also as a check on the accuracy of the simulation.

Section 5.2 presents results on the choice of a criterion for measuring performance of the system. The factors underlying choice of a criterion have been considered elsewhere.[2] The basic aim is to find a simple measure which will have the property of correlating with the performance of the system over a range of transmission facilities in the presence of impulse noise. It is shown that the aperture or opening of the "eye" pattern (see Fig. 7 of Section 5.2) is a reasonably satisfactory criterion. Therefore, the eye pattern is used for the presentation of results in the remainder of the paper.

Whenever applicable, general transmission design specifications are intertwined with the specific numerical results. Section 6.2 presents numerical results on the distortion produced when delay can be defined as a sinusoidal function of frequency. These results are interpreted to show general transmission design requirements for group (i.e., 40-kc or greater) bandwidths. Section 6.3 gives numerical results for the distortion effect of a variety of other delay shapes, for example, parabolic delay, as a function of frequency.

Sections 6.4 and 6.5 consider two general design questions. The first is: given some means of specifying allowable delay, that is, some class of transmission lines, find the line producing maximum degradation in performance. With this information one can then give bounds on performance, if bounds on the delay are specified. For a wide class of classical delay specifications, the result is essentially a two-cycle sinusoidal delay across the band. The next section considers the width of the band over which delay must be specified to predict system performance. It is shown that, for a system transmitting N bits per second, it is necessary to specify the delay over about $0.7N$ cycles of bandwidth, i.e., from the carrier $\pm 0.35N$ cycles.

Section 6.6 sums up the results on delay distortion to produce general transmission design specifications. The results are given in the form of curves of allowable delay vs maximum degradation. Three sets of curves are given to correspond to various shapes of delay in real facilities.

The final section gives some results for attenuation distortion. These latter results are not intended to be a systematic presentation, but show the magnitude of the effects.

III. SIMULATION TECHNIQUES

3.1 *Introduction*

This section considers those general simulation techniques appropriate to the study of a data transmission system. Many of these techniques were introduced by R. A. Gibby.[3] The main new approach is to introduce impulse noise to obtain the conditional probability of error given a noise of a specified nature present. The system is considered in blocks. For each block we attempt to duplicate mathematically the action the real system performs in shaping, or more generally in operating on, an electrical signal. This is not an attempt to duplicate the action of a particular capacitor or resistor but rather to present mathematically the performance of an entire system block. Further, advantage is taken of characteristics of certain system blocks to materially simplify the real system. For example, blocks in sequence which are commutative can be reversed without affecting the simulation results.

Fig. 1 shows two block diagrams of a data communications system. The upper figure is a common representation of a physical system. The lower figure is an equivalent model useful for simulation analysis. This equivalence is presented as an aid in understanding the nature of communication system simulation. Hereafter, we will call the upper figure the P (or physical) model and the lower figure the S model.

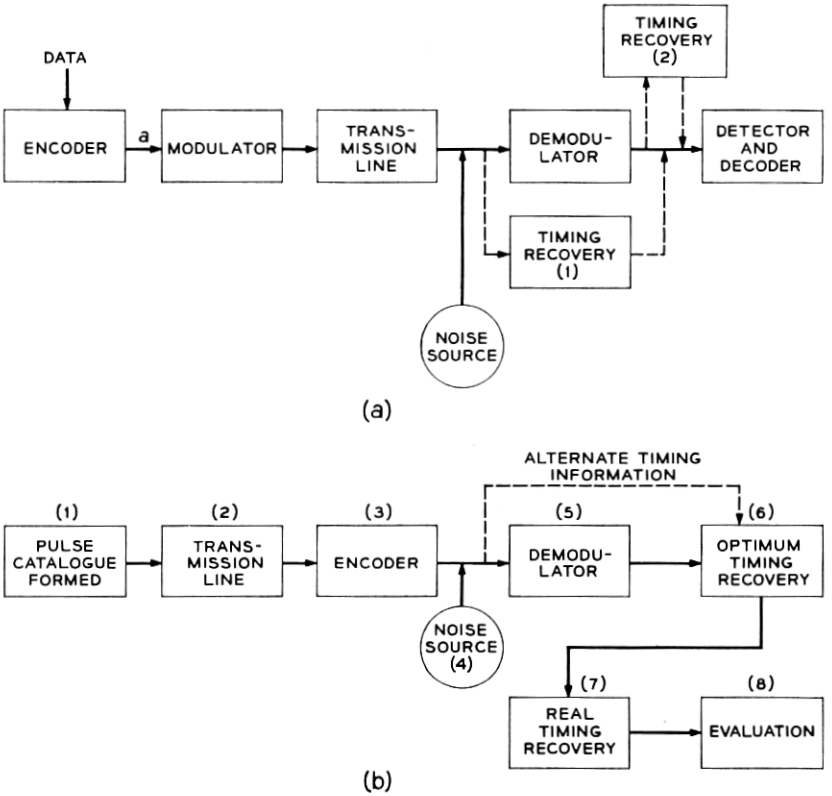

Fig. 1 — Block diagram representations of communications systems: (a) physical (P) model, (b) simulation (S) model.

3.2 *The Modulator and the Transmission Line*

The first box in the S model provides a catalog of all possible individual pulses used in the system. Since a digital computer is a discrete system, each pulse is defined by a sequence of sample values at a succession of evenly spaced time points. For a binary FSK system, for example, such a catalog would be one pulse each at the basic (mark and space) frequencies of the system.

The next step in the S model is to pass each pulse through the transmission medium. We emphasize that the pulses are acted on by the medium before they are encoded into a pulse train. This is justified by the commutative properties of filtering (i.e., action by the transmission medium) and adding together individual pulses displaced in time

(i.e., encoding of information). The third box in the S model then forms a pattern of pulses corresponding to the given pattern of encoded information.

The operation of the transmission facility on each pulse in the catalog is simulated in the frequency domain for reasons to be discussed shortly. Therefore, first a Fourier series of a particular pulse is formed in the computer. Next this Fourier series is modified by the attenuation and phase characteristics of the transmission facility. This operation will be discussed in greater detail in Section 5.3. The distorted pulses are then reformed in the time domain. These distorted pulses are then used to form a signal wave train corresponding to encoded information.

While the legitimacy of reversing blocks 2 and 3 follows from the commutativity of the two blocks, it is not yet clear why we should want to do this in a simulation. The basic motivation is the tremendous increase in speed when a simulation is performed in this way. Instead of having to process a long train of pulses through the transmission medium, it is now necessary to process only the small catalog of pulses inherent in the modulation technique. The superposition of the string of pulses is then a simple operation (which would in any case have to be done, no matter what the sequence of the blocks).

In addition, this approach gives a bonus of defining clearly individual pulses and their spectrums. We will see, in the section on sinusoidal delay distortion, the insight that is possible into performance of a system by the examination of individual pulses.

It is worthwhile to consider also why the transmission medium characteristics are simulated in the frequency and not the time domain. The underlying reason is that most practical knowledge of the plant is presently known in frequency domain parameters. By substituting for a Fourier approach a convolution of the impulse response of the line with each of the possible input signal pulses, a simulation can be easily modified to operate in the time domain. The advantages of reversing the sequence of boxes 2 and 3 of the S model hold just as strongly, and for the same reasons, in the time domain as in the frequency domain.

To make the greatest use of the long bit patterns available by simulating in this way, we desire a bit pattern that is representative of a random pulse train. What we actually use is what we will hereafter call a pseudo-random pulse train. For some integer h we desire to obtain every possible sequence of h bits the same number of times. For example, if h equals 3 there are eight possible combinations:

$$000,\ 001,\ 010,\ 011,\ 100,\ 101,\ 110,\ 111.$$

Any sequence in which each of these possible combinations of N

bits occurs exactly the same number of times will have the same distribution as a random sequence for all bit sequences of length up to and including N. For example, a sequence where each of the above occurs exactly once is given by

$$1\ 1\ 1\ 0\ 0\ 0\ 1\ 0\ 1\ 1.$$

A discussion of generation of such sequences can be found in Peterson.[4]

3.3 *The Demodulator*

Discussion of box 4, the introduction of noise into the simulation, will be postponed until later in this section. Box 5 of the S model represents the demodulator of the data transmission system. The signal processing of the demodulator is simulated on the computer. The basic approach is to duplicate the action of each block of the demodulator on the sequence of amplitude samples representing the data line signal. The output of the demodulator in the S model is then a sequence of amplitude samples representing the restored but distorted data pulse train.

Timing recovery in the S model is done in two separate steps. The first step, represented by box 6, is basically synchronization of the data train. The aim is to find the optimum sampling point relative to some criterion. Several criteria might be considered, but regardless of what criterion is used a synchronized or optimum timing point is obtained.

The second step in timing, represented by box 7, is to introduce the timing jitter which would occur in a physical system. Thus this box represents the physical timing recovery error, both that due to the jitter inherent in the circuits themselves and the jitter due to distortion of the data signal. The effect is to duplicate the degradation in performance due to imperfect timing. In keeping with methods used physically, the timing recovery signal can be generated either from the received line signal or the signal out of the demodulator.

3.4 *Noise Impairment — Performance Evaluation*

The last step in a simulation is to evaluate or measure the performance of the system. Some criterion of performance is chosen and is implemented in the simulation. For example, an eye pattern to measure system performance by the eye aperture might be formed. The eye pattern is formed by superimposing all possible three-bit intervals. In Fig. 7(a), a reference eye is shown. Fig. 7(b) shows some of the traces of a distorted waveform, and the resulting eye. The complete distorted eye would include all possible three-bit traces. The eye aperture is de-

fined as the minimax opening—that is, the maximum opening of the "worst" bit pattern. Various coding schemes can be introduced at this point, and the improvement they produce evaluated according to the chosen criterion.

We return now to discussion of box 4, the noise input, postponed in the previous presentation. Consider a noise burst of some particular size and shape introduced into a data system. We are interested in determining the conditional probability of error given this noise. In simulation the random occurrence of the noise pulse is replaced by the systematic introduction of a noise pulse at each of a large number of points in the data pulse train. As discussed above, the pulse train itself has each data sequence of a certain length, say 10 bits, occurring the same number of times; i.e., the possible sequences of N bits have uniform probability of occurrence. This pseudo-random data train is then mixed with noise by assuming the noise to be additive. Since a particular noise pulse is introduced at a very large (e.g., 4500) number of points, and uniformly along the data train, the effect is to introduce the noise randomly with uniform probability at all points in the data train.

The major difficulty in using an approach of this type is to choose noise pulse shapes which are representative of the telephone plant. In the mathematical sense this problem is at present unsolved. However, despite this present restricted knowledge, useful results are obtained for the following reasons. First, there is a range of system transmission conditions of interest for which relative performance is reasonably invariant under a range of different noise shapes. That is, although the absolute performance (i.e., the conditional probability of error) of each system changes from noise shape to noise shape, the relative performance, or ranking, of the systems stays the same over this range of noise shapes. Thus the degradation introduced by a particular transmission medium can be measured. Second, it is quite possible to handle a fairly large number of noise shapes. For example, in the four-phase case nine noise shapes were handled in quite reasonable computer times. Thus performance may be catalogued for various kinds of noise pending further knowledge. Finally, this implies a third basic use, which is that even if the system does perform differently under different wave shapes, this very information is useful in indicating both the basic nature of and possible improvements in a system.

The introduction of noise into the simulation can be used in various ways in measuring performance of the system. First, if the noise allows some ranking of transmission facilities, such as discussed in the paragraph above, it may be possible to directly correlate these rankings

with some criterion of performance of the system. This would then justify using this criterion in practice. For example, a justification for use of the eye aperture as a criterion for expected relative performance in four-phase transmission will be presented later. Second, it may be possible to use such a simulation in the design of better error detecting and correcting codes. That is, in the process of analyzing a long sequence of bits of a pseudo-random nature, it may appear that certain patterns of errors are more likely to occur in a realistic noise environment. Using such information, simpler error detecting and correcting codes on real lines might be obtainable. This is one approach to the construction of error codes on lines in which the memory is of a very complicated nature.

IV. FOUR-PHASE SYSTEM

4.1 *Physical*

We come now to the four-phase system which will be our prime concern for the remainder of the paper. The physical system we consider has been described by P. A. Baker.[1] The modulator of this system is shown in Fig. 2. Eight sine waves with the relative phases shown in the diagram are generated. These occur in two groups of four, as shown, and the data are encoded by choosing alternately from these two groups. The information is actually contained in the change in phase

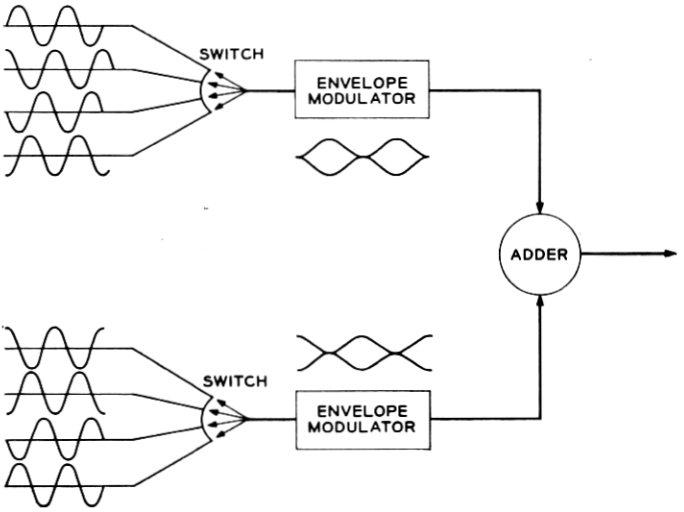

Fig. 2 — Modulator.

between successive pulses. Since each pulse encodes two bits of information, it has been given the name "dibit." The two alternating channels are used to insure there is always a change in phase between successive dibits. From the diagram it can be seen that this change is always one of four odd multiples of $\pi/4$. The actual shaping of the envelope of the sine waves is shown in the diagram. Just what this shaping should be to optimize performance was the first major check on the accuracy of the simulation. It will be considered in detail in Section 5.1.

The demodulator of the system is shown in Fig. 3. The information is recovered by comparing successive dibits to determine the change in phase between them. For this purpose the modulator uses two quite similar channels. We consider in detail only the upper one of the figure. The incoming signal is delayed by an interval of 1 dibit and then multiplied with the new incoming signal. This therefore results in a multiplication of successive dibit intervals. The output of the multiplier is then integrated. The result will be either positive or negative, depending on the relative phase of the two successive dibits. A truth table to recreate the encoded information is shown on the figure. This truth table

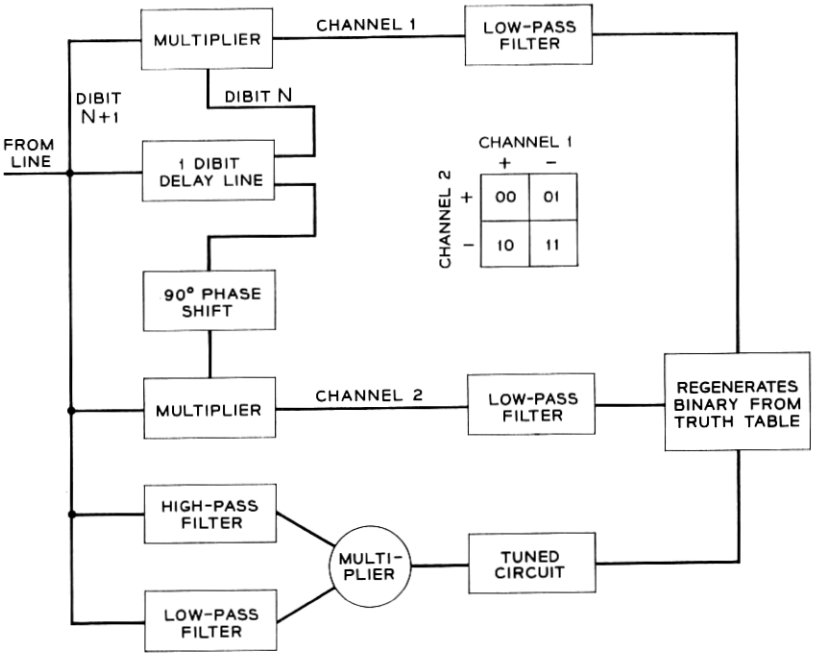

Fig. 3 — Receiver.

also demonstrates the result of the lower channel, which differs from the upper channel only in that it uses an extra $\frac{1}{4}$ cycle of delay. For greater detail the reader is referred to the paper by Baker.[1]

4.2 *Simulation*

This section is concerned with the application of the general techniques of simulation to the specific four-phase system. The simulation processes a data input train of 512 dibits. This corresponds to 1024 bits of input information, or to all possible combinations of four successive dibits. An extension of the exhaustive pattern technique mentioned above had to be developed for this four-phase case. It is no longer sufficient to make a choice between 0's and 1's for each information time slot. In the first time slot it is possible to pick any one of the eight possible signal waves, as shown in Fig. 2. Due to the alternation between the two channels of the modulator, it is possible to choose any one of four signals for each time slot after the first one. Thus, there are a total of $(8 \times 4 \times 4 \times 4 = 512)$ possible four-dibit combinations in the pseudo-random data train. For each sequence of four dibits there is another sequence different only in polarity; i.e., sequence A is simply the negative of sequence B. Since the multiplier eliminates this polarity difference, there is a seeming redundancy in using a pattern of this length. However, the noise introduced is of one polarity only. Thus this redundancy is necessary to obtain representative results with noise present.

There are two channels shown in the demodulator of Fig. 3. Initially both channels were simulated. It seems intuitively reasonable that the over-all results in these two channels should be essentially the same. For example, the signal sequence of initial phases -90, 45 should, with the extra 90° delay, give approximately the same results in the lower channel as the signal sequence 0, 45 gives in the upper channel. This is true within the limitations of slightly differing end effects between the two possible data sequences. There is such an image in the lower channel for every data sequence in the upper channel. One of the first tests performed with the working simulation was to check this hypothesis of approximately the same over-all results from the two channels. Over a fairly wide range of cases considered, no substantial difference in the performance of the two channels on an over-all basis was found. Therefore, the results given in this paper were obtained using only the upper channel of Fig. 3. The results apply to either channel operating alone, or to the system operating with both channels.

The results presented were obtained using nine basic noise wave-

shapes. These are shown in Fig. 4. In the first row are shown three sinusoidal pulses. These pulses differ in the ratio of their frequency to that of the dibit speed (or equivalently the carrier frequency) of the system. Similarly, the second row shows sinusoidal pulses subject to a one-sided exponential decay, and the third row shows two-sided exponentially decayed sinusoids. Each noise was considered over a range of noise to signal amplitudes. This range will be described more fully in Section 5.2. The noises shown were picked for two reasons. First, they represent a fairly wide range of parameters and shapes. Second, impulses idealized in this way are suggested by experimental studies of the telephone plant such as that of J. H. Fennick.[5]

V. BASIC SIMULATION RESULTS

5.1 *Simulation Check — Envelope Shaping*

The first step in using a simulation must be to check its performance against the physical model it represents. In the case of four-phase simulation this first check was provided by an investigation of the optimum envelope shaping (in some particular class of functions) in the modulator.

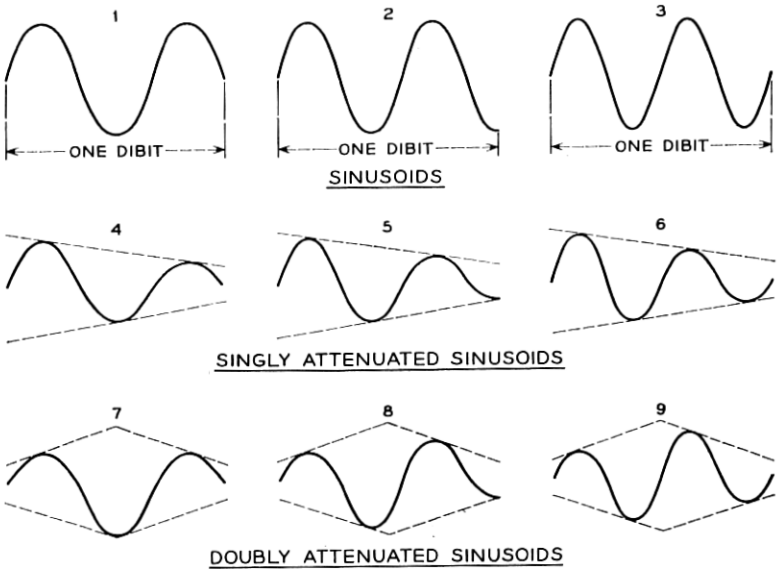

Fig. 4 — Noise waveshapes; all shapes are shown prior to detection but subsequent to transmission.

Prior to the envelope shaping the basic four-phase pulse is given by

$$f(t) = \sin [\omega_{car}t + n(\pi/4)] \qquad n = 0,1,2,3,4,5,6,7 \tag{1}$$

where n represents the information content of the wave. Consider first a raised-cosine envelope shaping. Then a four-phase pulse is denoted by (upper indicates upper channel of modulator)

$$\begin{aligned} f_{upper}(t) &= \sin\left(\omega_{car}t + n\frac{\pi}{4}\right)\left[\frac{1}{2} + \frac{1}{2}\cos\frac{\omega}{2}\,\text{dibit}^t\right] \qquad n = 0,2,4,6 \\ f_{lower}(t) &= \sin\left(\omega_{car}t + n\frac{\pi}{4}\right)\left[\frac{1}{2} - \frac{1}{2}\cos\frac{\omega}{2}\,\text{dibit}^t\right] \qquad n = 1,3,5,7 \end{aligned} \tag{2}$$

A typical sequence of such pulses is shown in Fig. 5(a). However, as can be seen in Figs. 2 or 5(a), this full raised-cosine envelope builds in an overlap between successive dibits. One alternative to such shaping is phase shift keying—that is, a jump from one phase to another at dibit intervals. However, since the transmission lines have finite bandwidth, such phase jumps would be distorted in transmission. To provide a controlled smooth transition, rather than the uncontrolled distortion resulting from the action of finite bandwidth on phase jumps, while minimizing the effect of the built-in overlap of the raised cosine, the basic functional form of the envelope given by (3) was considered

$$\begin{aligned} \text{env}_{upper}(t) &= \frac{\frac{1}{2}\cos\frac{\omega_d t}{2} - \frac{1}{2}\cos\frac{\omega_d T}{2}}{\frac{1}{2} - \frac{1}{2}\cos\frac{\omega_d T}{2}} \qquad 0 \leqq \left|\frac{\omega_d t}{2}\right| \leqq T\pi \\ &\qquad\qquad \tfrac{1}{2} \leqq T \leqq 1 \\ &\qquad\qquad T\pi \leqq \left|\frac{\omega_d t}{2}\right| \leqq \pi \\ &= 0 \\ &\qquad\qquad \omega_d = \text{dibit radian frequency} \end{aligned}$$

and similarly for the lower channel envelope. The parameter T controls the amount of built-in overlap of the modulation envelope. The optimum value for T agreed when found independently in a laboratory test of the working system by Baker and on the computer. This provided a check on the simulation.

The optimum value of T is $\frac{3}{4}$. This corresponds to a modified raised cosine with about $\frac{1}{4}$ dibit overlap, as shown in Fig. 5(b) (that is, about 50 per cent of the maximum overlap of Fig. 5a). The shaping of this modulation envelope in effect determines the amplitude spectrum of the line signal. In the course of subsequent investigation on the computer, another class of amplitude shaping was also considered. A typical mem-

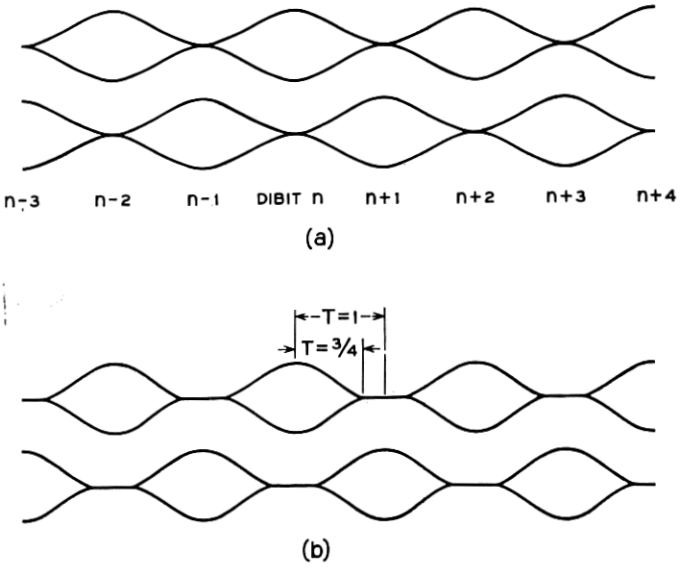

Fig. 5 — Envelope shaping: (a) full raised-cosine shaping, (b) modified shaping used in present data terminals.

ber of this class of squared-off raised-cosine amplitude spectra is shown in Fig. 6 along with the spectra resulting from a complete raised-cosine shaping (that is $T = 1$) and for the optimized $T = \frac{3}{4}$. A sequence of values of the parameter b (see Fig. 6) of the squared-off raised cosine was considered. No value of b gave performance as good as the modified raised cosine with $T = \frac{3}{4}$.

5.2 *Criterion — Eye Pattern*

The measure of performance used in obtaining the results described in the above paragraph was the eye pattern (Fig. 7). However, while the accuracy of the simulation can be checked by comparing the eye obtained in a laboratory test to that obtained by the simulation, this does not in itself justify the eye as a suitable measure of performance for the four-phase data system. This justification of the eye depends in the final analysis on demonstrating a correlation between the expected performance of the system in a real noise environment and the opening or aperture of the eye.

Impulse noises of nine different shapes were introduced into the simulation. Each of these was considered over a signal-to-noise ratio of about 14 db, from noise of +5 to −9 db relative to the signal. The

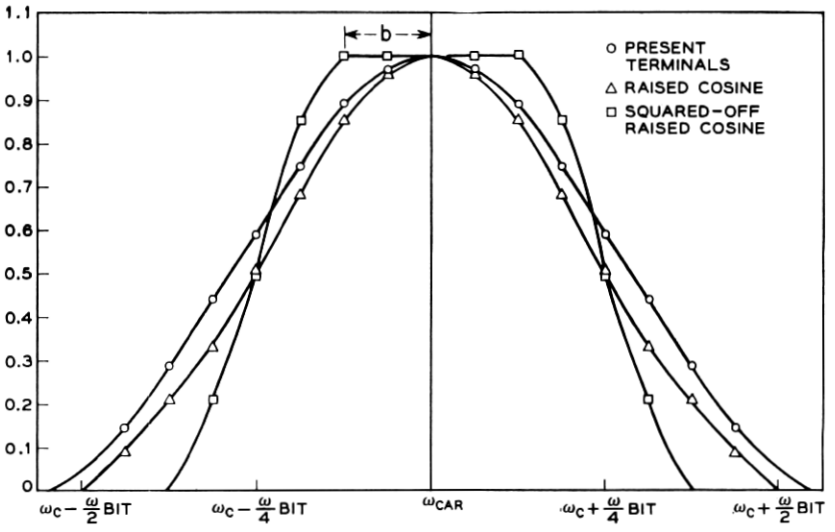

Fig. 6 — Envelopes of amplitude spectra.

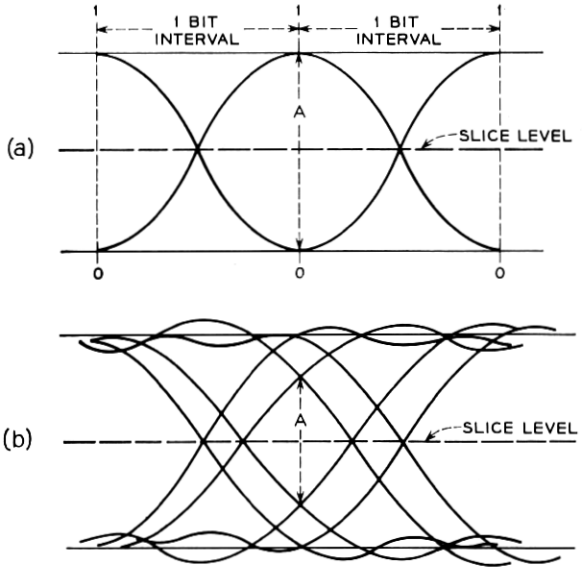

Fig. 7 — Eye patterns. (a) Undistorted eye: tracings result from patterns 000, 001, 010, 011, 110, and 111; A is eye aperture normalized for undistorted eye to 1.0. (b) Distorted eye: figure shows some tracings; total eye formed from *all* possible three-bit intervals.

signal-to-noise ratio was defined as the peak undistorted signal amplitude relative to the peak noise amplitude.

The arbitrary nature of this definition is not significant, since it does not affect the ranking or relative performance of various lines. A sample of the many cases considered is shown in Fig. 8 for two noises and two transmission lines (one of which is back-to-back or reference transmission). As might be expected, all of the lines perform approximately the same at very high noise levels. At such levels the noise completely swamps out the signal, and the resulting performance is then the totally random effect of the noise alone. We therefore choose the range of conditional probability of error for which the results are meaningful in terms of degradation in performance. To avoid misunderstanding, we note that while performance is certainly sensitive to noise waveshape,

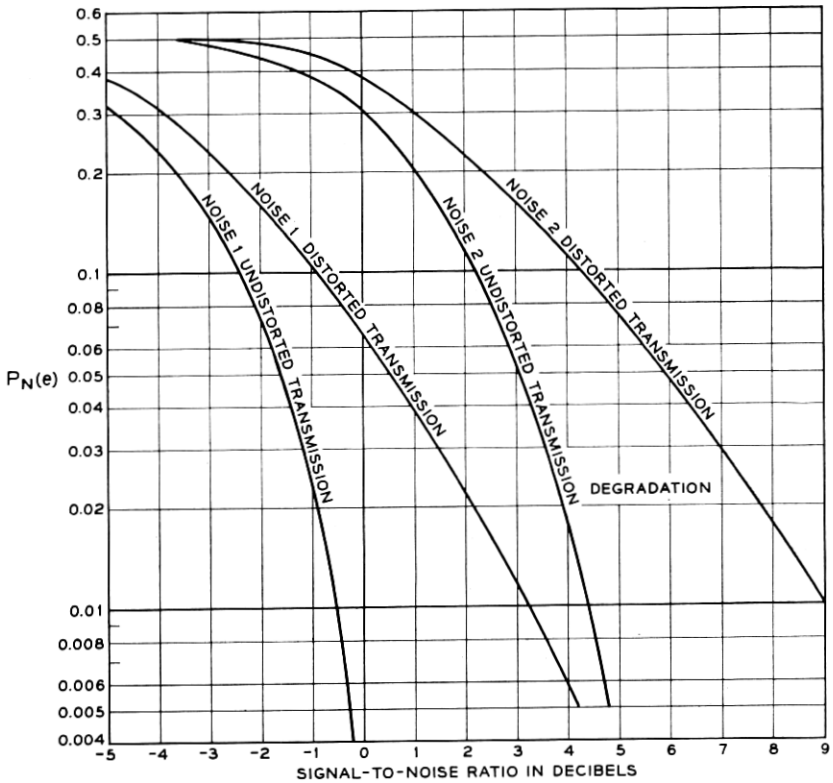

Fig. 8 — Conditional probability of error $|P_N(e)|$ vs S/N [db (peak undistorted signal/peak noise)]. Shows results of two sample noises on a distorted and an undistorted transmission line.

much of the difference seen in Fig. 8 comes from defining S/N using the peak value, and not some average total power measure for the noise.

The range of conditional probability of error chosen for these tests was between 0.005 and 0.125. For a particular transmission line and conditional probability of error, there is a range of degradation of performance as measured by the change in signal-to-noise ratio for various noise shapes. A sample of the noise results obtained is given in Table I for a range of transmission lines in the following manner. First the transmission line is described with a sufficient number of parameters to characterize it. For example, sinusoidal delay is described in terms of its amplitude (Bm), its frequency (m) and its phase θ relative to the transmission band. A detailed discussion of each parametric representation will be described later. Numerical results are then given for each of three levels of conditional probability of error, namely 0.005, 0.025, and 0.125. These results are the range in degradation and signal-to-noise ratio due to the nine noises considered for the given transmission line relative to back-to-back performance. The correlation in performance between results obtained using conditional probability of error and the eye aperture can be seen by comparing the degradation in performance measured by successively smaller $P(e)$ (i.e., for successively smaller noises) with the degradation measured by the aperture shown in the last column. It is seen that the eye seems to give a limiting value.

Figs. 11–13 of Section 6.2 are presented in terms of eye aperture. Presentation in this form is justified by the fact that, for the range of transmission lines and noise considered, the value of eye aperture correlates consistently with the degradation in performance obtained by keeping constant conditional probability of error. This justification is one of the principal results of this paper. While this does not demonstrate that the eye will be a good measure of performance for all possible distortions, the wide range of noises and transmission facilities considered indicates the eye to be an appropriate criterion for four-phase transmission, at least over lines whose principal distortion is nonuniform delay.

5.3 *Transmission Line Simulation*

A typical four-phase data pulse is given by the product of $f(t)$ of (1) and envelope (t) of (3). As mentioned previously, passing these pulses over a transmission line was done in the simulation in the frequency domain. Thus for each of these pulses a Fourier series was formed. A typical example of such a series is given in (5), where ω_0, the fundamental frequency of the Fourier series, determines the spacing of the spectral lines which represent the wave:

TABLE I—RANGES OF CONDITIONAL PROBABILITY OF ERROR

All numbers are degradation in db relative to no distortion—range represents variation over nine noises.

Delay	Degradation (in db) Measured Using Conditional Probability of Error			Degradation (in db) Measured Using Aperture
	$P(e) = 0.125$	$P(e) = 0.025$	$P(e) = 0.005$	
Sinusoidal				
$Bm = 0.5$, $m = 0.5$, $\theta = \pi/2$	0–0.3	0.5–0.8	0.7–1.2	1.1
1.5 0.5 0	1.4–1.8	3.1–3.7	3.8–4.5	4.9
1.5 0.5 $\pi/2$	2.9–3.5	6.2–6.6	8.2–8.9	9.6
1.0 1 0	1.3–1.7	3.1–3.8	4.2–5.0	4.8
1.0 1 $\pi/2$	2.8–3.7	6.4–7.0	8.6–9.3	10.2
1.0 1.25 $\pi/2$	3.0–3.8	7.1–7.6	9.7–10.5	11.7
0.5 1.5 0	0.6–1.0	1.8–2.2	2.5–3.1	3.1
1.0 1.5 0	3.9–4.4	8.5–8.8	11.4–11.7	12.8
1.0 1.75 0	4.5–5.1	9.8–10.5	13–14.5	15.8
0.5 2.0 $\pi/2$	0.3–0.7	1.5–1.8	2.1–2.8	3.1
1.0 2.0 $\pi/2$	2.0–2.7	5.6–6.3	8.1–9.0	10.1
1.5 2.5 0	5.6–6.1	12.1–12.7	17.5–19.0	24.5
Parabolic				
1.0 bit delay at $\omega_{car} \pm 0.35\ \omega_{bit}$	0.3–0.4	1.1–1.2	1.6–1.9	1.8
1.5 bits delay at $\omega_{car} \pm 0.35\ \omega_{bit}$	0.8–1.0	2.1–2.5	3.3–3.4	3.7
1.5 bits delay at $\omega_{car} + 0.275\ \omega_{bit}$ $\omega_{car} - 0.425\ \omega_{bit}$	1.1–1.7	3.2–3.7	5.0–5.1	5.8
1.5 bits delay at $\omega_{car} + 0.2\ \omega_{bit}$ $\omega_{car} - 0.5\ \omega_{bit}$	2.5–3.1	6.6–6.8	10.3–11.3	12.4
Quartic				
1.25 bits delay at $\omega_{car} \pm 0.35\ \omega_{bit}$	0.2–0.8	0.8–1.3	1.7–2.2	1.9
1.25 bits delay at $\omega_{car} + 0.275\ \omega_{bit}$ $\omega_{car} - 0.425\ \omega_{bit}$	0.7–1.3	2.5–2.7	3.5–4.0	4.8
1.0 bit delay at $\omega_{car} + 0.2\ \omega_{bit}$ $\omega_{car} - 0.5\ \omega_{bit}$	2.1–2.6	5.3–5.8	8.5–9.8	11.3
Band cutoff cases				
Quadratic delay to $\omega_{car} \pm 0.35\ \omega_{bit}$ — then delay uniform	0.6–0.9	1.4–1.7	2.3–2.5	2.5
Delay of Fig. 22, curve a	2.0–2.8	4.6–5.0	7.8–8.4	8.8
Delay of Fig. 22, curve c	1.1–1.6	3.6–3.8	5.2–5.9	6.3
Delay of Fig. 22, curve f	1.0–1.2	2.6–2.8	3.5–4.0	4.4
Attenuation cases				
Sinusoidal delay				
$Bm = 1.0$, $m = 2.5$, $\theta = 0$ 6-db slope atten. of Fig. 9(a)	2.4–3.2	5.2–6.0	7.8–8.5	8.9
Sinusoidal delay				
$Bm = 0.5$, $m = 2.0$, $\theta = 0$ 6-db slope atten. of Fig. 9(a)	2.6–3.2	4.6–6.2	7.5–8.1	9.9

$$f(t) \text{ env } (t) = g(t) \tag{4}$$

$$g(t) = \sum_{n=0}^{N} A(n\omega_0) \cos [n\omega_0 t + \psi(n\omega_0)]. \tag{5}$$

$A(n\omega_0)$ and $\psi(n\omega_0)$ are the amplitude and phase of the spectrum of the pulse across the transmission band of interest. The effect of passing such a pulse through a transmission medium is to yield an output pulse which can be represented by:

$$h(t) = \sum_{n=0}^{N} A(n\omega_0)\ R(n\omega_0) \cos [n\omega_0 t + \psi(n\omega_0) + \varphi(n\omega_0)]. \tag{6}$$

Here, $R(n\omega_0)$ and $\varphi(n\omega_0)$ represent the attenuation and phase of the transmission medium. The envelope delay $D(\omega)$ is the derivative of $\varphi(\omega)$ with respect to ω.

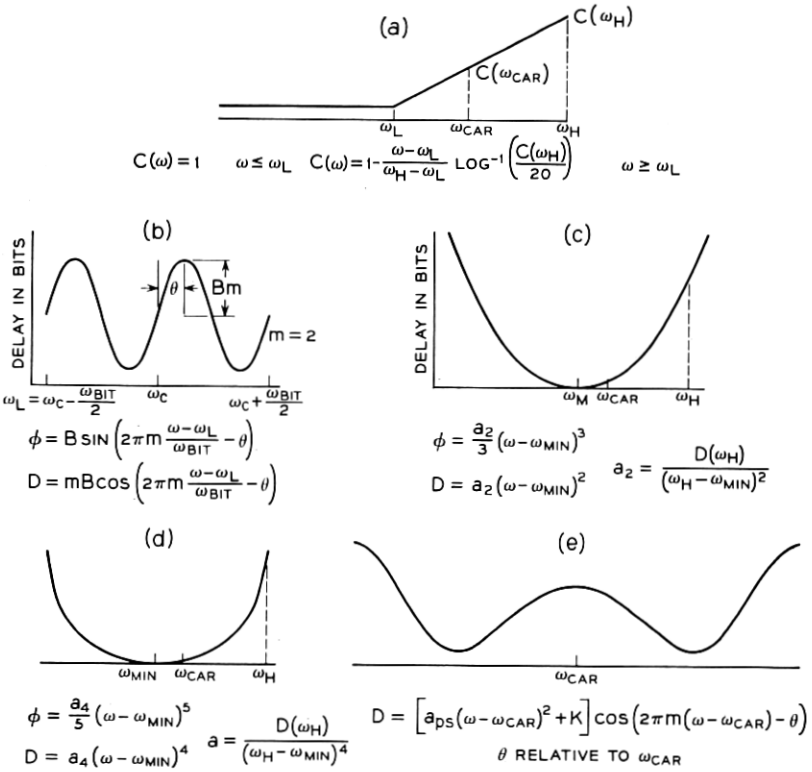

Fig. 9 — Attenuation and delay shapes.

The parametric forms of $R(\omega_0)$ and $D(\omega)$ are given in chart form in Fig. 9. Aside from a flat passband, the primary form of attenuation considered was one which seems to be typical of a large part of the voice-band plant. It consists of a flat passband out to some cutoff frequency, followed by a slope attenuation of so many db per cycle. We note that this is not db per octave; that is, the curve is linear with respect to frequency and not with respect to the log of frequency. In addition, some attenuations previously introduced, whose spectra are shown in Fig. 6, were also considered. Among these is the effect of varying the built-in overlap or intersymbol interference, which is, of course, also a variation in the amplitude spectrum of the pulses.

The general forms of delay considered were sinusoidal, parabolic, quartic and a parabolic bounded sinusoid. In addition, many of these forms were also used with variations in the band edges of the delay. For example, sinusoidal delay might be used across 70 per cent of the band and then a relatively sharp cutoff delay used at the band edge. Finally the simulation is set up to handle frequency by frequency read-in of both phase and attenuation across the transmission band.

VI. DELAY RESULTS

6.1 *Introduction*

The remainder of this article is a presentation of the results achieved using the simulation to investigate performance of a four-phase system over a telephone channel. While some raw data results on impulse noise are presented in Table I, for the reasons described above the remainder of the discussion will refer to the eye aperture results shown in curve form in a group of figures.

6.2 *Multicycle Sinusoidal Delay — Group Band Transmission Design*

We begin our discussion with the results obtained in an application which is at once the simplest to explain, has perhaps the clearest intuitive explanation of the effects of delay, and yet is of definite practical importance. This is the case illustrated in Fig. 9(b), in which the delay is a sinusoidal function of frequency across the transmission band of interest.

Such a sinusoidal delay is defined in terms of three parameters. First is the amplitude of the delay (*Bm* of the figure), which characterizes the peak delay in bit times. Second is the phase (θ), which represents the position of the sinusoidal delay relative to the carrier frequency of the system. Finally, the number of cycles of the sinusoid

across the transmission band of interest is given by m. This characterization is of particular interest in group bands. Typical delay shapes which arise due to group band separation filters might be those shown in Fig. 10(a). In order to permit transmission of data over group band channels these delay curves are equalized. The results of equalization typically yield a number of cycles of sinusoidal delay, such as shown in Fig. 10(b). The designer often has some control both over the magnitude and the number of ripples of delay, with a compromise to be made between technical factors and economics. That is, the greater the number of ripples required, in general, the more stages of equalization are needed, and thus there is an economic constraint involved.

The basic results on multicycle sinusoidal delay are shown in Figs. 11 through 13, where Fig. 13 is an overlay of the preceding two figures. A number of conclusions can be drawn from these results. For design

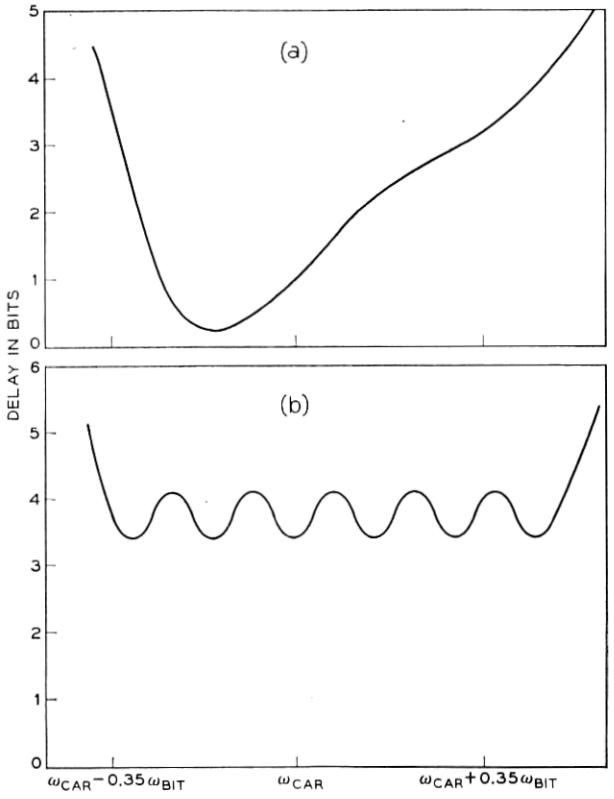

Fig. 10 — Group bands: (a) unequalized, (b) equalized.

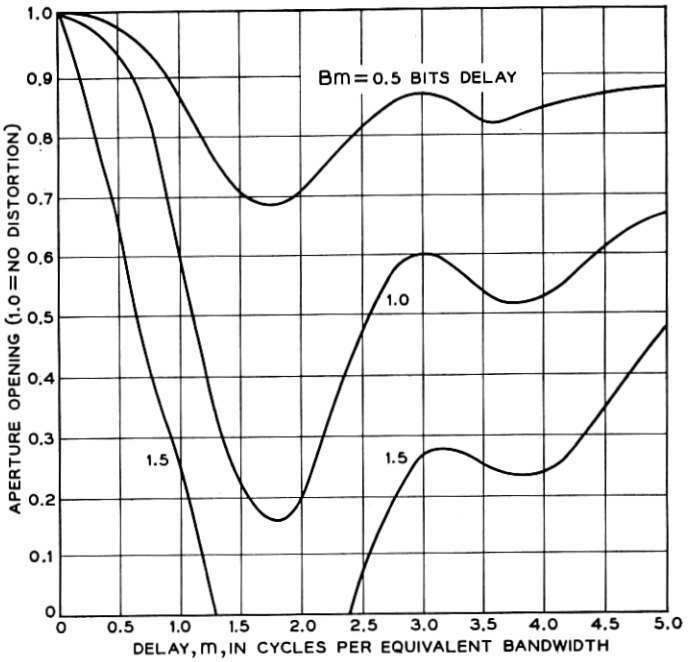

Fig. 11 — Aperture vs delay for sinusoidal delay; all curves use $\theta = 0$,

$$D = \frac{Bm}{\omega_{bit}} \cos\left[\left(\frac{\omega - \omega_c}{\omega_{bit}}\right)m + \theta\right].$$

Aperture = 0 indicates system makes errors even with no noise. Peak-to-peak delay = $2Bm$. Curves for Bm = 0.5, 1.0, and 1.5 bits peak delay.

purposes, two of these are most significant. First is the general improvement in transmission as the number of cycles of delay is increased while holding the peak delay in dibits constant. Second is the relative preference for an odd number of cycles of delay across the passband. This is clearest if $\theta = 0$ (i.e., the aperture for $m = 3$, $\theta = 0$ is larger than for $m = 4$, $\theta = 0$). If $\theta = \pi/2$ there is not much difference between $m = 3$ and $m = 4$. However, since the larger m will generally be more expensive to achieve by equalizing, $m = 3$ would again be preferred.

We consider first the improvement in transmission for constant peak delay. To a first-order approximation this can be explained on the basis of echo theory.[6] Since the delay is sinusoidal, the interference introduced is due primarily to echoes. In particular, simulation shows the first echo on each side of the pulse transmitted to be the primary cause of interference. The amplitude of any echo is proportional only to the

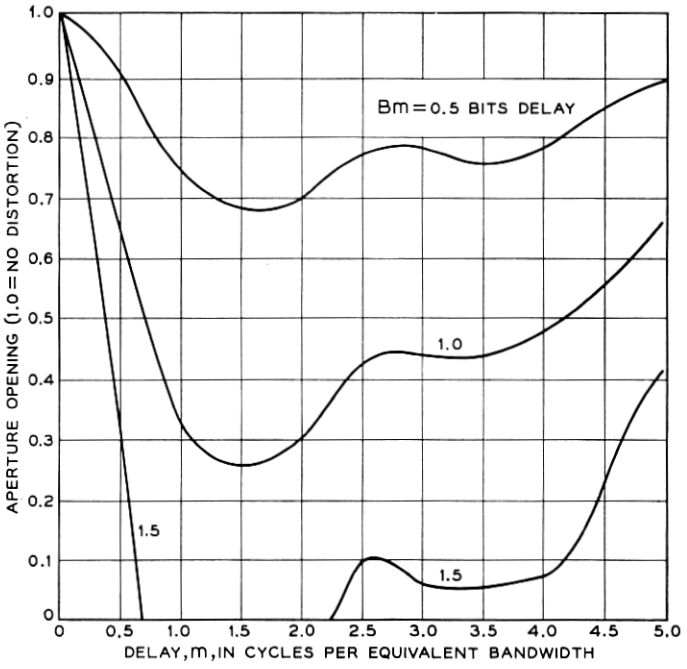

Fig. 12 — Aperture vs delay for sinusoidal delay; all curves use $\theta = \pi/2$,

$$D = \frac{Bm}{\omega_{\text{bit}}} \cos\left[\left(\frac{\omega - \omega_c}{\omega_{\text{bit}}}\right) m + \theta\right].$$

Aperture = 0 indicates system makes errors even with no noise. Peak-to-peak delay = $2Bm$. Curves for Bm = 0.5, 1.0, and 1.5 bits peak delay.

amplitude of the sinusoidal phase (B), and is independent of the other parameters of the delay. Thus as the number of cycles of sinusoidal delay increases, holding the product Bm constant, B decreases and so does the interference. Fig. 14 shows a typical four-phase system pulse and the echoes produced by the sinusoidal delay for various numbers of cycles (in frequency) with constant peak delay. The advantages of the simulation being able to show individually distorted pulses in such clear detail is most evident at this point.

On the other hand, the position of the echo is determined solely by the number of cycles of sinusoidal delay across the band; that is, the distance of the echo from the main pulse is directly proportional to m. The preference for odd numbers of cycles of delay can be explained, to a first-order approximation, as follows. The primary interference is the first echo in each direction. As the number of cycles of delay increases,

the effect on this echo is to move it farther and farther from the main pulse. We note that the amplitude of the echo is decreasing for a constant value of peak delay. In practice, this means that as the number of cycles of delay is increased, the interference progressively phases in and out with respect to the time at which the demodulated pulses are sampled. In other words, while the echo is always present, its major point of interference oscillates between the sampling instant and midway between the sampling instants of the demodulated pulse train. This oscillating phasing in and out with respect to the sampling time of the interference from the echo produces alternately more and less interference at the sampling instants.

An example is shown in Fig. 14. The peak of the first echo comes midway in the adjacent time slots of the two-cycle interference. This produces a maximum distortion in phase in the adjacent time slot —

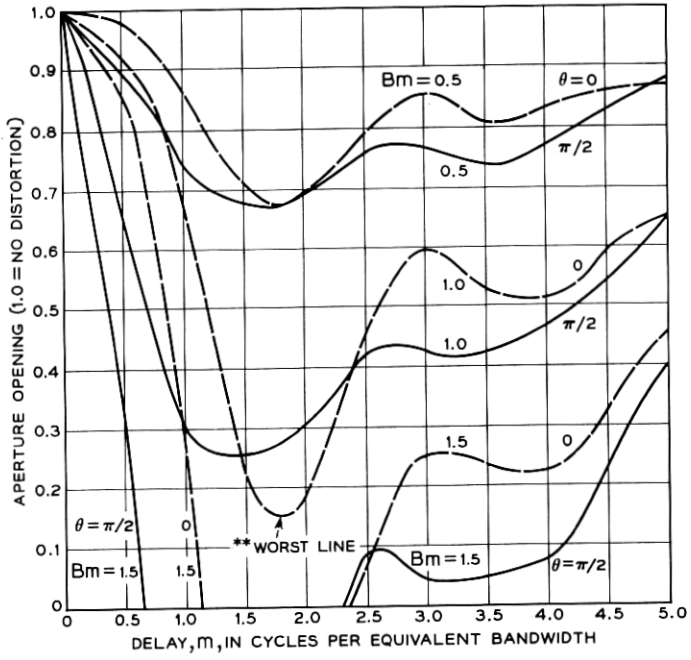

Fig. 13 — Combination of Figs. 11 and 12:

$$D = \frac{Bm}{\omega_{bit}} \cos\left[\left(\frac{\omega - \omega_c}{\omega_{bit}}\right) m + \theta\right];$$

aperture = 0 indicates system makes errors even with no noise; peak-to-peak delay = $2Bm$.

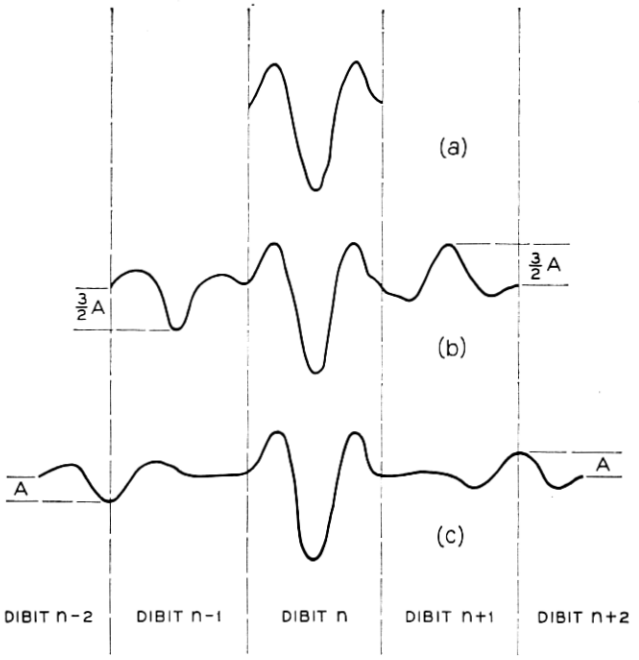

Fig. 14 — Effects of sinusoidal delay in terms of echoes: (a) basic four-phase pulse, (b) echoes from two-cycle/band sinusoid, and (c) echoes from three-cycle/band sinusoid.

that is, at the sampling instants. For the three-cycle interference, the echo reaches a peak midway between time slots. It therefore produces less distortion in either of the two time slots it interferes with, and a correspondingly lower maximum distortion.

6.3 *Delay Results Useful for Voice-Band Design*

This section introduces and discusses results over a variety of delay characteristics. The curves representing these characteristics share the property that they have no more than 3 minima. Their general shapes are such that they can be made to represent a wide variety of voice-band channels.

The first set of curves, shown in Fig. 15, is simply an enlargement of the effects of sinusoidal delay for less than two cycles of sinusoid. Fig. 16 shows some typical voice-band delay curves. For each an approximating sinusoid (with its associated parameters) is given. The results in Fig. 15 are for θ from zero to $\pi/2$ radians. However, since the

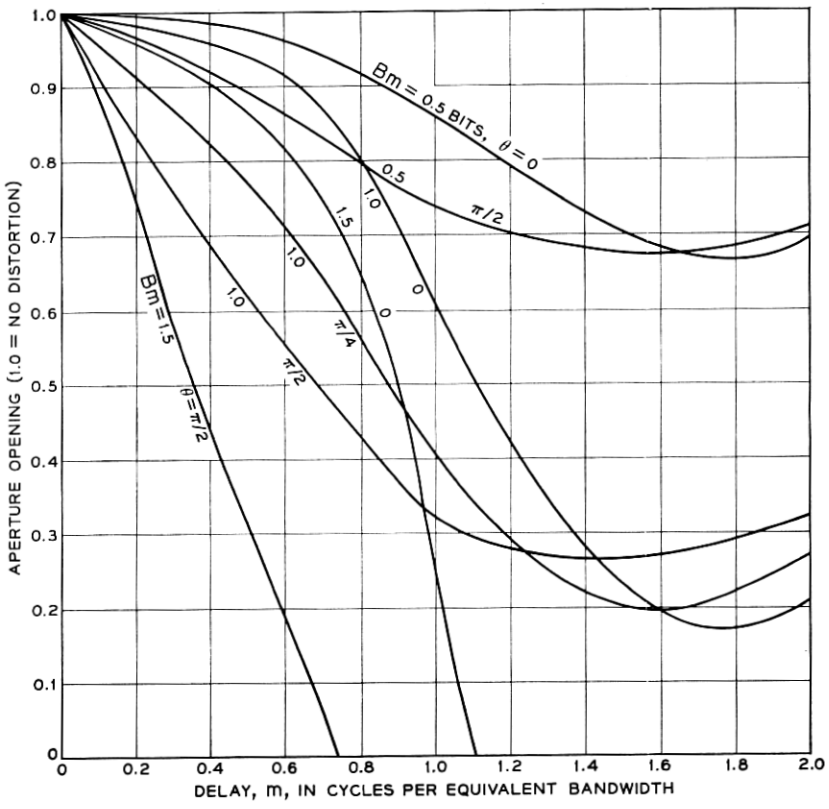

Fig. 15 — Aperture vs delay for sinusoidal delay — expansion for low m of Fig. 13.

$$\text{Delay} = \frac{Bm}{\omega_{bit}} \cos\left[\left(\frac{\omega - \omega_c}{\omega_{bit}}\right) m + \theta\right].$$

Aperture = 0 indicates system makes errors even with no noise present; peak-to-peak delay = $2Bm$.

results repeat in successive quadrants (i.e., $\theta = \pi$ gives essentially the same results as $\theta = 0$) the curves represent the full range of θ.

Figs. 17 and 18 give results for quadratic and fourth-power delay distortion. The curves represent delay symmetric with respect to the carrier, and displaced from the carrier by varying percentages of the bandwidth of interest. It is worthwhile to note again that these curves are, as are all the curves given in the results, normalized with respect to the carrier frequency and the bit speed. Thus one can apply the results to any frequency range and corresponding bit speed. The curves are

normalized for a $1\frac{1}{2}$ carrier cycle per dibit system. Thus, for example, a typical system at this speed would have an 1800 cycle carrier and transmit 2400 bits per second, i.e., 1200 dibits per second. Again, the same curves apply to a 48,000-bps system using a 36-kc carrier.

The results presented to this point represent relatively simple delay shapes—that is, sinusoidal, quadratic, or quartic delays. It will be shown in Section 6.5 that the same results apply within very reasonable limits to any delay curve which is identical with one of the delays considered over a minimum of 70 per cent of the band. In addition one class of relatively complicated delay shapes was also investigated. These delays are parabolically bounded sinusoids, and are described in Fig. 9(e). As the product of a parabola plus a constant with a sinusoid they can be used to represent a wide class of various delay shapes. The results are given in Figs. 19 and 20 for $m = 2$ and $m = 3$ and for a range of values of the ratio α_{ps} to K. It will be seen that these ratios are particularly

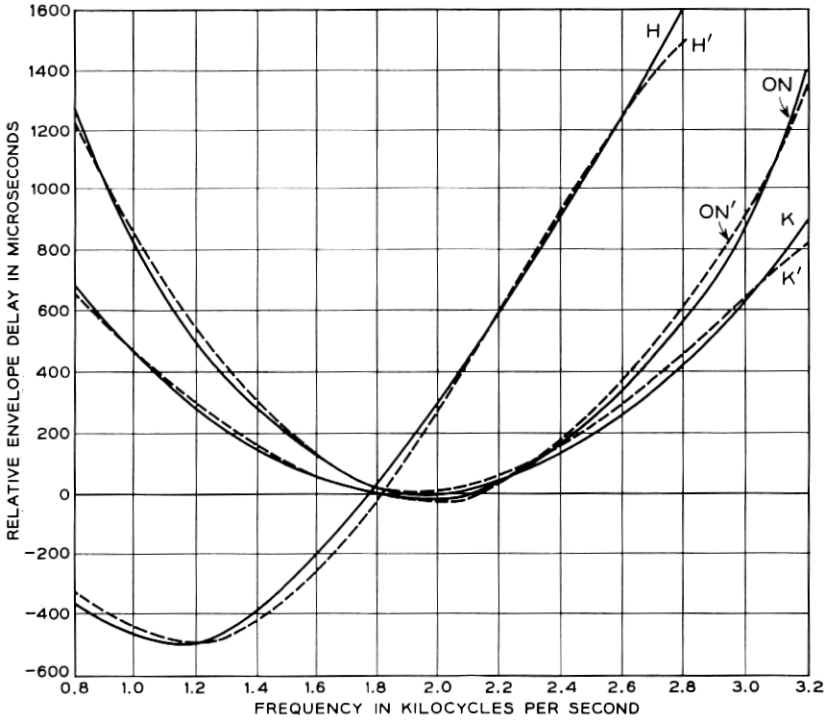

Fig. 16 — Representations of some typical lines by sinusoidal approximations (primes are approximations). K = 2 links K carrier, ON = 3 links ON carrier, and H = 300 miles of H44 loaded cable.

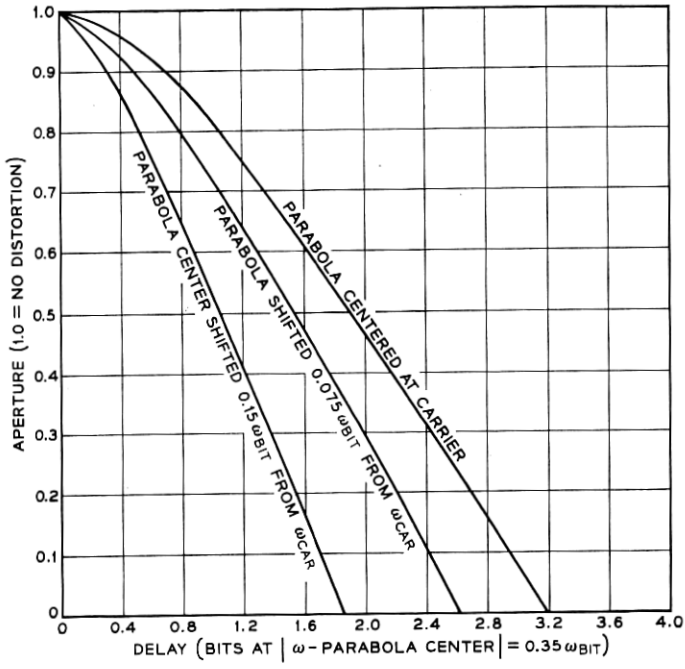

Fig. 17 — Apertures for parabolic delay; aperture = 0 indicates system makes errors with no noise.

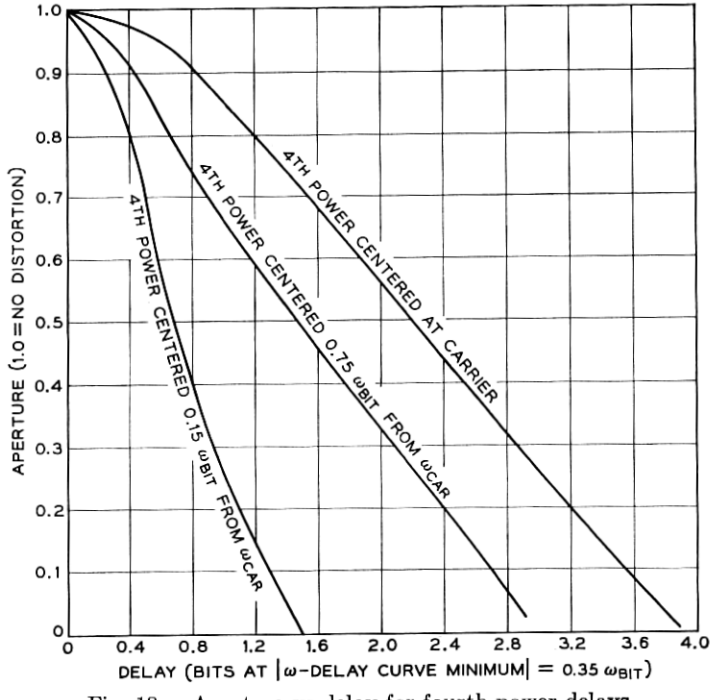

Fig. 18 — Aperture vs delay for fourth-power delays.

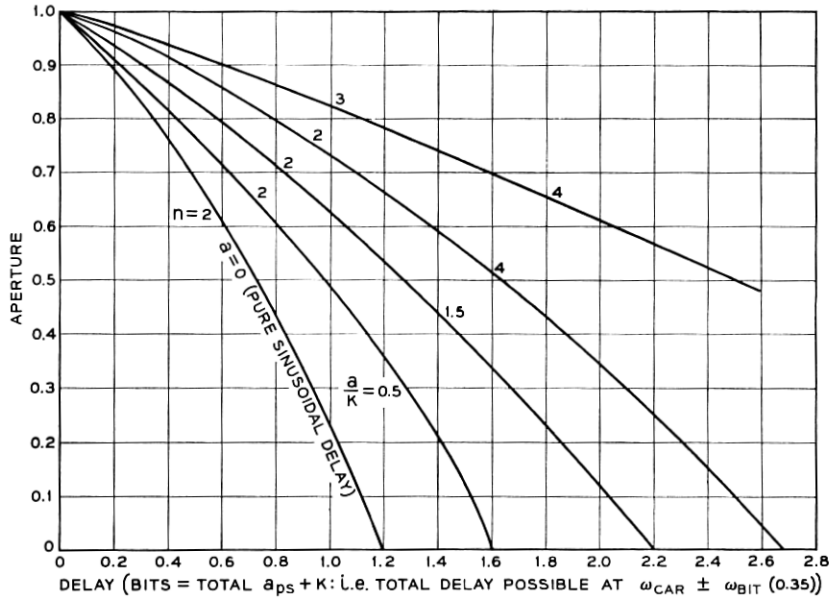

Fig. 19 — Aperture vs delay for parabolic bounded sinusoidal delays, $\theta = 0$.

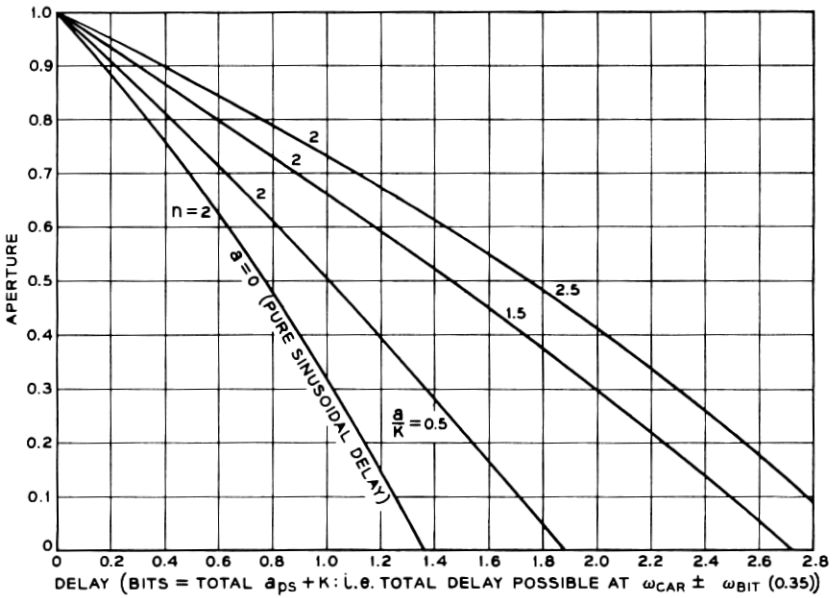

Fig. 20 — Aperture vs delay for parabolic bounded sinusoidal delays, $\theta = 90°$.

useful in the setting of curves of maximum degradation for performance in the voice band.

6.4 *Line in a Given Class Producing Most Degradation*

The simplest generally used way of characterizing delay is to specify the maximum allowable delay across some percentage of the transmission band. For example, one might say that the maximum delay across 70 per cent of the transmission band is to be no more than $\frac{1}{2}$ dibit (making a tacit assumption that the minimum delay is 0). It is of interest to specify the worst possible delay shape meeting such a requirement — that is, to find the delay shape falling within this allowable maximum which produces the worst degradation in performance. For a line of reasonably good performance, say for eye openings greater than 0.6, an answer to this problem has been provided by R. W. Lucky.[7] However, since the lines he allows include such pathologies as discontinuities in the delay, the limiting cases must often for our purposes be considered nonrealizable. It is therefore of interest to find the worst line out of the classes we have considered, using the above criterion of "worst." For a check this worst line then can be compared to that obtained by Lucky.

If the limiting value of delay is defined across 60 per cent of the band or greater, the worst performance in the classes discussed above is that obtained with a slightly less than two-cycle sinusoid across the transmission band. Fig. 21 shows in graphic form the difference in performance between such a two-cycle sinusoid and various other delay characteristics having the same maximum delay across a given percentage of the band. For the range of reasonably good transmission lines which Lucky has considered, Lucky's "worst" line produces only about one db greater degradation in performance as measured by the respective aperture values (or equivalently by the impulse noise performance; see Section 5.2) than this two-cycle sinusoid. When one remembers that Lucky's lines are in general quite drastic in their shapes, it seems reasonable to use this two-cycle sinusoid as an upper bound through the remainder of this paper.

6.5 *Effect of Delay at the Edges of the Band*

Examination of the spectrum of an individual pulse shows that the energy falls off very rapidly toward the edge of the band. Now when timing is performed using the line signal, the energy near the sides of

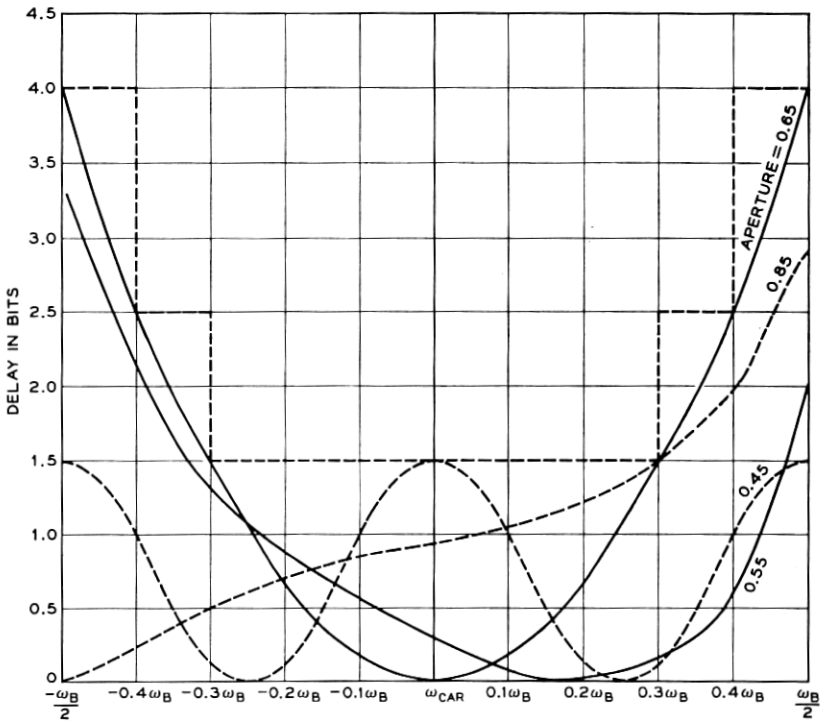

Fig. 21 — Examples of performance range meeting classical delay requirements; frequency in multiples of bit speed from carrier.

the band can (and for certain nonrandom patterns does)* contain a great deal of the necessary information. On the other hand, for timing performed from the data signal, in general for timing from random data, and for recovery of the data itself, the edges of the band contain only a relatively small amount of the information. Thus it would not appear necessary to specify the delay as accurately across the entire transmission band of interest.

A number of delay curves were used to check this supposition. Fig. 22 shows some of the cases which gave the widest variation in performance. These lines have respectively quadratic (curves a, b, c) and fourth-power (curves d, e, f) delay as a function of frequency for the frequency range $\omega_{car} - 0.35\ \omega_{bit}$ to $\omega_{car} + 0.35\ \omega_{bit}$. However, the eye apertures

* Timing for random patterns even when using the line signal gets most of its energy from the center of the band where the spectrum has much greater amplitude. This fact was pointed out to the author by M. A. Logan.[8]

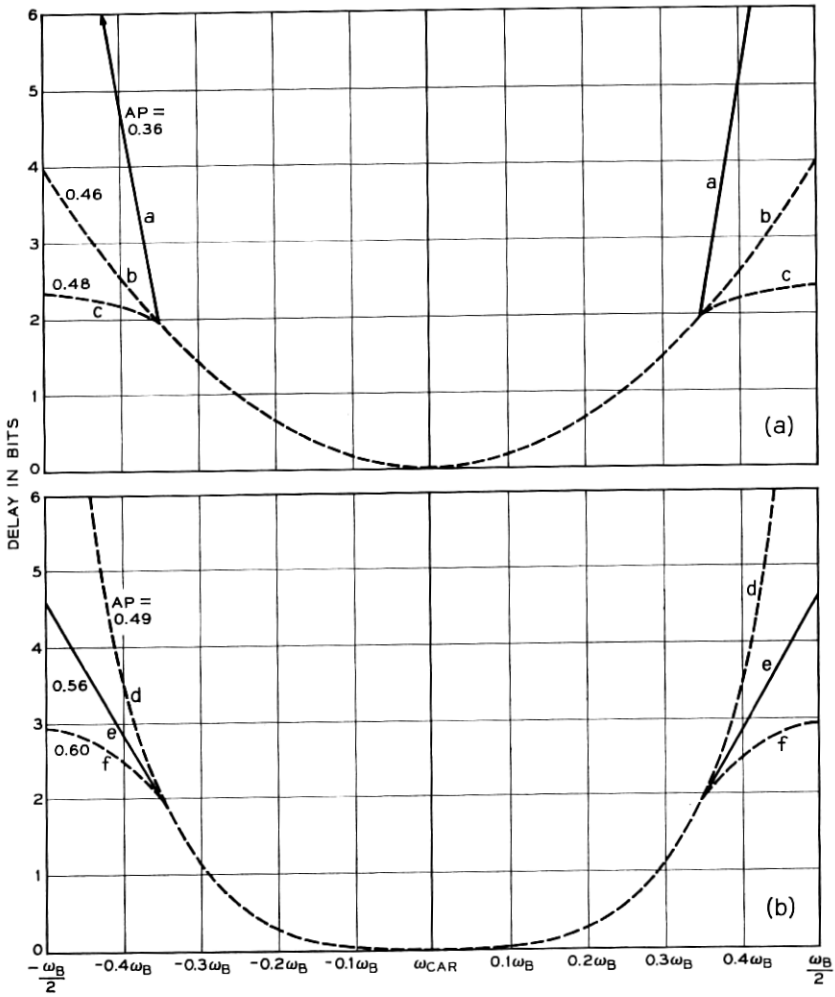

Fig. 22 — Bandwidth requirements, all curves symmetric about ω_{car} : (a) quadratic delay, (b) fourth-power delay.

for even the extreme cases shown vary by less than 2 db, and in most cases that seem to be of practical interest a variation of less than one db was found. The same results held for the impulse noise performance discussed in Section 5.2.

Similar results were found for delays in which the center band delay was a sinusoidal or parabolically bounded sinusoidal function of frequency. Therefore, one concludes that if delay is specified for the frequency range from $\omega_{car} - 0.35\ \omega_{bit}$ to $\omega_{car} + 0.35\ \omega_{bit}$, then for the

recovery of the data signal it is not worth the cost or effort to try to equalize delay beyond about 70 to 75 per cent of the transmission band.

6.6 *Voice-Band Transmission Design*

Historically, the specification of delay has been given in a staircase arrangement. This is equivalent to setting a sequence of pairs of check frequencies and the limitation on delay between them. Thus, for example, a typical delay specification might be

$$\begin{aligned} &\omega_{car} - 0.3\ \omega_{bit}\ \omega_{car} + 0.3\ \omega_{bit} && 1.5 \text{ dibits delay} \\ &\omega_{car} - 0.4\ \omega_{bit}\ \omega_{car} + 0.4\ \omega_{bit} && 2.5 \text{ dibits delay} \\ &\omega_{car} - 0.5\ \omega_{bit}\ \omega_{car} + 0.5\ \omega_{bit} && 4.0 \text{ dibits delay.} \end{aligned} \tag{7}$$

When delay is specified in this manner, no account is taken of the wide variation in performance of delays of various shapes all meeting the basic requirements. Thus, for example, the delays shown in Fig. 21 all meet the requirements listed above, yet have eye apertures ranging from 0.45 to 0.85. In effect, one is faced with the choice of either placing too strict a requirement for many delay shapes, or not in truth being able to guarantee that delays meeting a particular requirement will have no more than a certain allowable degradation.

These results suggest a somewhat more complicated specification of delay requirements for good transmission design. One way of doing this is to use a single equation and vary the parameters of this equation to allow for various delay shapes — for example, to bound the delay by $\alpha_{ps}\ \omega^2 + K$. By choosing various ratios of α_{ps} to K one can allow for a wide variety of delay shapes.

In the voice band there are three major shapes of delay which must be considered: namely, the usual single-minimum parabolic-type delay shape which arises from carrier transmission, the slope-type delay which arises from loaded cable, and the more rectangular delay with a ripple across the transmission band which results from equalizing. The three curves of Fig. 21 are examples of these types of curves. To represent these classes, consider three values of the ratios of α_{ps} to K. For the equalizer ripple-type line a ratio of α_{ps} to K of 1 to 1 was chosen. For a carrier transmission delay a ratio of α_{ps} to K of 4 to 1 was taken. For the loaded cable-type delays a ratio of 8 to 1 was chosen. For each of these delay shapes a set of design curves for various allowed degradations was derived. In each case the maximum delay was found such that a specified degradation in performance would not be exceeded. As usual, the allowable degradation is in aperture or equivalently in impulse noise performance. These curves are shown in Figs. 23, 24 and 25.

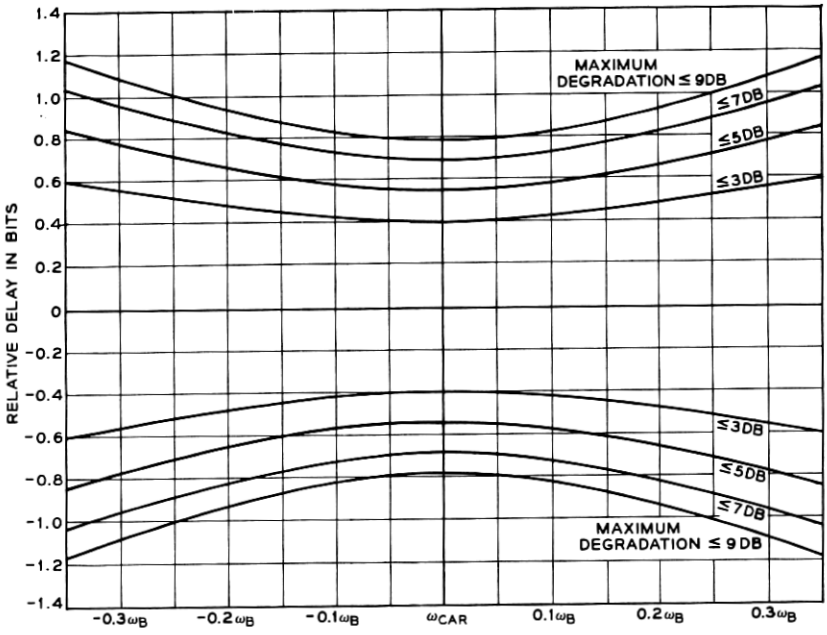

Fig. 23 — Design curve no. I. Maximum allowable delay for $\alpha_{ps}/K = 1$ to give indicated degradation:

$$D = [\alpha_{ps}/(\omega - \omega_{car})^2 + K] \cos (nw + \theta).$$

Curves give maximum degradation; in general, degradation should be less for delays falling within bounds shown. Note that flat delay introduces no distortion.

It is not necessary for the delay of a particular line to meet all the requirements of all three sets of curves in order to have a particular allowable degradation. On the contrary, if a given delay falls within any one curve for a particular allowable degradation in performance then it will meet this degradation requirement. Thus, in the field or in design, it is necessary to consider three curves of allowable delay to determine if a particular delay shape will meet a particular degradation requirement.

In the curves, delay has been specified only up to 70 per cent of the band. This is in keeping with the previous results on the non-necessity of specifying delay beyond this point. However, it is true that there is some range in the actual performance due to the effect of delay beyond the 70 per cent limit. In addition, as discussed in the section on worst lines, these delays are not the actual worst lines as found by Lucky. To allow for these two factors, an additional 1-db margin is built into each of the curves. It is felt that only in the very rarest of circumstances

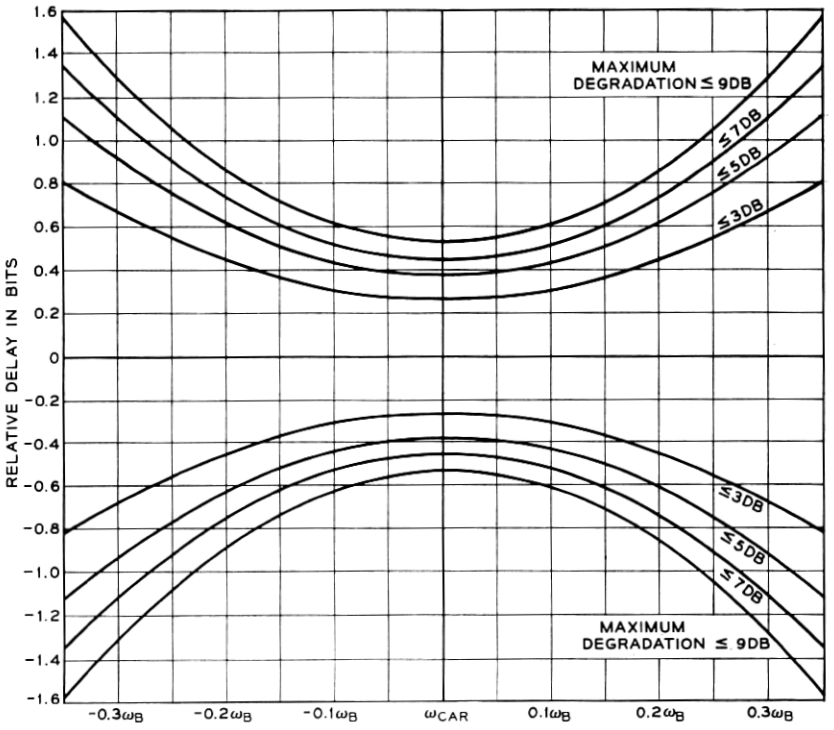

Fig. 24 — Design curve no. II. Maximum allowable delay for $\alpha_{ps}/K = 4$ to give indicated degradation:

$$D = [\alpha_{ps}/(\omega - \omega_{car})^2 + K] \cos (nw + \theta).$$

Curves give maximum degradation; in general, degradation should be less for delays falling within bounds shown. Note that flat delay introduces no distortion.

will this margin be insufficient, and then only by a very small additional amount of degradation.

VII. ATTENUATION RESULTS

The scope of this study did not include a systematic investigation of the distortion due to attenuation alone or to a combination of attenuation and delay. However, certain representative results are discussed here to indicate some of the effects of attenuation. The simulation can, of course, handle any desired attenuation.

The spectrum has symmetric components with respect to the carrier. Thus for symmetric delay (in particular for no delay distortion), slope attenuation across the transmission band [i.e., attenuation = k_1 (frequency) + k_2] should produce an effect equivalent to a flat loss of value

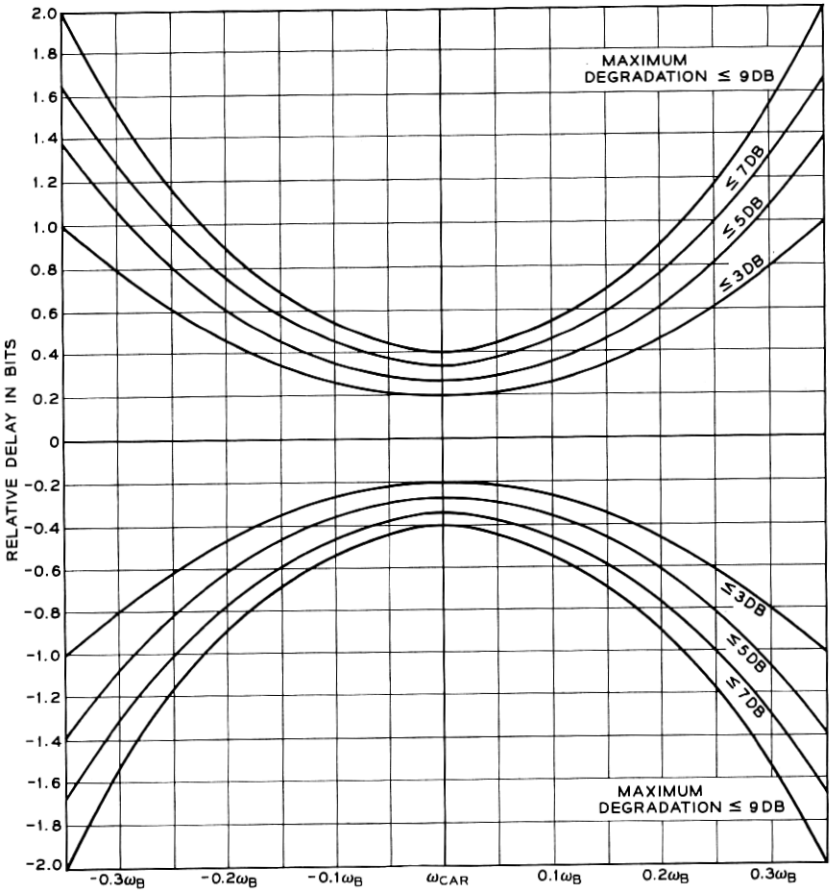

Fig. 25 — Design curve no. III. Maximum allowable delay for $\alpha_{ps}/K = 8$ to give indicated degradation:

$$D = [\alpha_{ps}/(\omega - \omega_{car})^2 + K] \cos (nw + \theta).$$

Curves give maximum degradation; in general, degradation should be less for delays falling within bounds shown. Note that flat delay introduces no distortion.

equal to the attenuation at the carrier frequency. This line of thought was essentially verified using the simulation. In the presence of delay unsymmetrical with respect to the carrier frequency, however, this is no longer true. This also indicates the nonadditive nature of the effects of attenuation and delay. In any study of the combined effects of attenuation and delay distortion, it is this nonadditive nature of the interaction which is the most important single fact.

The general form of attenuation considered was linear on a plot of db versus frequency as shown in Fig. 9(a). This attenuation shape was found to be typical of voice-bands by Alexander, Gryb, and Nast.[9] The cutoff frequency was taken as the carrier minus 20 per cent of the bit speed. For example, with an 1800-cps carrier operating at 2400 bps, this would be at 1800 − (0.2) (2400) = 1320 cps. The slope was measured from this cutoff frequency ($\omega_{car} - 0.2\ \omega_{bit}$) to $\omega_{car} + 0.35\ \omega_{bit}$. Slopes ranging from 4 to 12 db over this range were investigated.

Table II shows clearly the nonadditive interaction of the attenuation plus delay. Both delays shown in Table II are sinusoidal and respectively of odd and even symmetry with respect to the carrier frequency. The results are normalized to zero attenuation at the carrier.

TABLE II — INTERACTION OF ATTENUATION AND DELAY

Amplitude	Delay		Attenuation	Aperture Delay Only	Aperture Delay + Attenuation
Bm	θ	*m*	6-db slope	0.45	0.36
1.0	0	2.5			
Bm	θ	*m*	6-db slope	0.70	0.32
0.5	$\pi/2$	2.0			

VIII. ACKNOWLEDGMENTS

As in almost every paper it is really impossible to give credit to all those who have contributed to the author's understanding of the problem. However, special thanks are due to R. A. Gibby for guidance and motivation and for introducing the author to the simulation approach to problems of this type. In addition, R. R. Anderson, R. W. Lucky and S. Habib in analysis and simulation, M. A. Logan and P. A. Baker in the area of the physical system, and H. C. Fleming, D. W. Nast, and W. R. Young in the area of transmission design were particularly helpful in the development of this paper.

REFERENCES

1. Baker, P. A., PM Data Sets for Serial Transmission at 2000 and 2400 Bits per Second, Conference Paper CP-62-143, A.I.E.E., Fall, 1961.
2. Rappeport, M. A., Criterion Problem in Data Transmission, Conference Paper 63-534, A.I.E.E., Winter, 1963.
3. Gibby, R. A., An Evaluation of AM Data System Performance by Computer Simulation, B.S.T.J., **39**, May, 1960, p. 675.
4. Peterson, W. W., *Error Correcting Codes*, John Wiley & Sons, New York, 1961.
5. Fennick, J. H., A Report on Some Characteristics of Impulse Noise in Tele-

phone Communication Systems, Conference Paper 63-986, IEEE, June, 1963.
6. Wheeler, H. A., The Interpretation of Amplitude and Phase Distortion in Terms of Echoes, Proc. I.R.E., **27,** June, 1939, p. 359.
7. Lucky, R. W., A Functional Analysis Relating Delay Variation and Intersymbol Interference in Data Transmission, B.S.T.J., **42,** Sept., 1963, p. 2427.
8. Logan, M. A., private communication.
9. Alexander, A. A., Nast, D. W., and Gryb, R. M., Capabilities of the Telephone Network for Data Transmission, B.S.T.J., **39,** May, 1960, p. 431.